Environmental Modelling and Software 108 (2018) 186–196

Contents lists available at ScienceDirect

Environmental Modelling & Software

journal homepage: www.elsevier.com/locate/envsoft

Estimating daily meteorological data and downscaling climate models over landscapes

Miquel De Cáceres[a,b,*], Nicolas Martin-StPaul[c], Marco Turco[d], Antoine Cabon[a,b], Victor Granda[a]

[a] Forest Sciences Centre of Catalonia (CTFC), Solsona, 25280, Spain
[b] Center for Ecological Research and Forestry Applications (CREAF), Cerdanyola Del Vallès, 08193, Spain
[c] Ecologie des Forêts Méditerranéennes, INRA, F-84914, Avignon, France
[d] University of Barcelona, Department of Applied Physics, Av. Diagonal 647, Barcelona, 08028, Spain

ARTICLE INFO

Keywords:
Bias correction
Climate change
Drought stress
Statistical downscaling
Regional climate model
Weather interpolation

ABSTRACT

High-resolution meteorological data are necessary to understand and predict climate-driven impacts on the structure and function of terrestrial ecosystems. However, the spatial resolution of climate reanalysis data and climate model outputs is often too coarse for studies at local/landscape scales. Additionally, climate model projections usually contain important biases, requiring the application of statistical corrections. Here we present 'meteoland', an R package that integrates several tools to facilitate the estimation of daily weather over landscapes, both under current and future conditions. The package contains functions: (1) to interpolate daily weather including topographic effects; and (2) to correct the biases of a given weather series (e.g., climate model outputs). We illustrate and validate the functions of the package using weather station data from Catalonia (NE Spain), re-analysis data and climate model outputs for a specific county. We conclude with a discussion of current limitations and potential improvements of the package.

1. Introduction

Regional climate-driven impact studies, such as those in forest ecological and hydrological research, rely increasingly on spatially- and temporally-high resolution climatic data. For example, evaluating the impact of climate on functions and services of forest ecosystems using process-based models often requires daily meteorology as input (e.g., Davi et al., 2006; De Cáceres et al., 2015; Granier et al., 2007; Ruffault et al., 2013). However, employing spatially-coarse climatic projections drawn from global databases in impact studies can lead to substantial errors (e.g., Patsiou et al., 2014; Randin et al., 2009). Even relatively fine-grained (i.e. 1 km) climate products (Hijmans et al., 2005) do not always rely on all the available surface station data. As a consequence, the surface meteorology of areas with complex terrains may be inadequately described, leading to irrelevant inferences of ecological patterns at local scale (Bedia et al., 2013).

The tasks needed to obtain data at fine temporal (daily) and spatial (< 1 km) resolutions are different for observed climate than for climate projections and may depend on the size of the target area and the available data. Daily meteorological data for a single target location may be obtained from weather sensors installed on-site. Historical data series for the target location may be obtained by comparing the estimates of the recently-installed on-site sensors with those of a nearby weather station having longer records, or with daily reanalysis data extracted from global or continental databases (Dee et al., 2011; Hofer et al., 2010; Turco et al., 2014; Weedon et al., 2011). For a large topographically-heterogeneous area, however, installing sensors may be too expensive, and fine-grained weather estimates may be obtained by spatial interpolation of records from weather station networks (Goovaerts, 2000; Li and Heap, 2014; Wagner et al., 2012). Different R functions and packages already exist to access daily weather station data (Iannone, 2015) or to calculate radiation in a complex topography (Brenning, 2008); and broad range of options exist to interpolate weather variables, using either deterministic approaches such as splines or stochastic methods such as kriging (Gräler et al., 2016). One of the current limitations from the perspective of climate impact modeler, however, is the lack of platforms providing an integrated interface from which conduct easy and fast spatial interpolation for a given temporal period and a set of relevant weather variables simultaneously.

Regarding climate projections, different methodologies have been

Abbreviations: CDF, Cumulative distribution function; GCM, Global climate model; MAE, Mean average error; MAP, Mean annual precipitation; RCM, Regional climate model

* Corresponding author. Centre Tecnològic Forestal de Catalunya. Ctra. antiga St. Llorenç km 2, E-25280, Solsona, Catalonia, Spain.
E-mail address: miquelcaceres@gmail.com (M. De Cáceres).

https://doi.org/10.1016/j.envsoft.2018.08.003
Received 18 September 2017; Received in revised form 10 March 2018; Accepted 3 August 2018
Available online 04 August 2018
1364-8152/ © 2018 Elsevier Ltd. All rights reserved.

developed to bridge the gap between the spatial resolution of Global Circulation Models (GCMs) and local observations (Sunyer et al., 2015; Winkler et al., 2011). One approach to obtain climate change predictions at reasonably fine resolution is through dynamical downscaling, which consists on running a high-resolution Regional Climate Model (RCM) driven by GCM outputs (or reanalysis data) within a limited domain. RCMs provide, to a certain degree, physically consistent output at regional scale and allow nowadays reaching spatial resolutions varying from 10 to 50 km (Jacob et al., 2014; Kotlarski et al., 2014). Although RCMs provide additional spatial detail compared to GCMs, RCM resolution may still be too coarse to satisfy the needs of landscape- or local-scale studies (Kendon et al., 2012; Winkler et al., 2011). Moreover, RCM climate projections can have considerable biases (including those inherited from GCM forcing) that preclude their widespread and direct use (Glotter et al., 2014; Ruffault et al., 2014). Thus, generally RCMs cannot be directly used as input for impact models unless some form of statistical correction/calibration is performed (Christensen et al., 2008; Kotlarski et al., 2014; Turco et al., 2013). Another approach to reach the local scale is statistical downscaling, which is based on empirical relationships established between larger–scale variables (e.g., mean sea level pressure) and local records in the region of interest (e.g., precipitation in a number of stations) (Benestad et al., 2008). The application of statistical techniques on GCM or RCM outputs is also meant to address model biases and requires calibrating transfer functions where local weather data are compared with model outputs for a reference period (Maraun et al., 2017b, 2010; Winkler et al., 2011).

During the last decade, downscaling has become a strategic topic in international and national climate programs and, as a result, substantial improvements in statistical and dynamical downscaling have been obtained and are currently under development (Kotlarski et al., 2014; Maraun et al., 2017a). There exist data repositories and tools for accessing GCM and RCM outputs (Palma, 2017) and several R packages specifically designed to perform and evaluate statistical downscaling in its different forms (Bedia et al., 2015; Benestad et al., 2017; Gudmundsson, 2016; Hanel et al., 2017). However, generally there is still a gap between climate data providers and impact user needs regarding the choice and parameterization of downscaling procedures, potentially limiting the possibility to estimate the climate-driven impact uncertainties (Harris et al., 2014; Rössler et al., 2017). One solution to this problem would be to involve downscaling specialists in every climate-driven impact study (Maraun et al., 2017b). Another, perhaps more strategic, solution is to promote the development of interdisciplinary collaborative tools that guide decisions of impact researchers by providing access to a selection of robust and sound downscaling and correction procedures.

Here we present *meteoland*, an R package created to facilitate the estimation of observed and future daily weather at any position over complex terrains. Specifically, the package allows the user: (a) to interpolate daily weather records, including topographic corrections and the calculation of incident solar radiation and potential evapotranspiration; (b) to statistically correct the biases of weather series, such as those given by climate models. The main advantage of *meteoland* over existing R packages is that it covers the full chain of climate data manipulation (e.g. Fig. 1), helping users to obtain the suitable input needed for ecological impact studies in an easy and integrated way. While it currently implements a few among all the options available to perform these tasks, it is our intention to continue developing the package as a collaborative project between climate researchers and climate impact modelers.

In section 2, we describe how daily meteorological data is represented in the package, and briefly explain how the interpolation and correction routines work (detailed information can be found in the package itself). After that (section 3), we illustrate the main functions of the package: (3.1) the calibration and validation of interpolation routines for the region of Catalonia (NE Spain); (3.2) the interpolation of daily weather at 1ha resolution across Solsonès, a county within Catalonia; (3.3) the examination of the effect of correcting climate model predictions across Solsonès, using either coarse resolution re-analysis data (0.5° ~ 50 km) or fine resolution interpolated data (1 km) as reference; and (3.4) an examination of the corresponding effects in an impact model focused on simulating soil water balance and tree drought stress within forest stands. We finish (section 4) by briefly discussing limitations of the package and potential improvements.

2. Package description

2.1. Data structures and main functions

R package *meteoland* deals with the estimation of the following daily surface weather variables (units in parentheses): Mean, maximum and minimum temperature (°C); precipitation (mm = $l \cdot m^{-2}$); mean, maximum and minimum relative humidity (%); incident solar radiation ($MJ \cdot m^{-2}$); wind speed ($m \cdot s^{-1}$) and wind direction (degrees from North) at 2-m height. Building on data structures of the sp package, meteoland works with three kinds of spatial structures: points, grid pixels and full grids. Class **SpatialPointsMeteorology** is suited to store temporal meteorology series at specific locations. It extends **SpatialPoints** in that it includes one data frame for each point, where rows correspond to dates and weather variables are in columns. Each of these data frames is stored in the disk in the form of a separate (.txt or.rds) file, and point coordinates are stored in an additional metadata file. Classes **SpatialPixelsMeteorology** and **SpatialGridMeteorology** are suited for storing and mapping daily meteorology over a partial or a full spatial grid, respectively. These classes extend **SpatialPixels** and **SpatialGrid** objects, respectively; and contain one data frame for each date, where rows are grid cells and columns are weather variables. **SpatialPixelsMeteorology** and **SpatialGridMeteorology** objects are stored in the disk using the netCDF format, using the *ncdf4* R package (Pierce, 2017).

Functions 'interpolationpoints', 'interpolationpixels' and 'interpolationgrid' perform the spatial interpolation of weather on a set of target points, a subset of grid cells or a full spatial grid, respectively. Similarly, 'correctionpoints' allows correcting the meteorological series of a set of points. Calculations can be done either having all data stored in memory or by reading/writing meteorological data every time it is needed, a feature that becomes critical when processing a large number of points or grid cells. Table 1 lists these and other functions that are included in meteoland.

2.2. Spatial interpolation

A large number of methods have been proposed for the interpolation of daily meteorology, particularly for precipitation (Daly et al., 2002; Dodson and Marks, 1997; Goovaerts, 2000; Liston and Elder, 2006; Thornton et al., 1997), and several studies have evaluated and compared their performance (Dirks et al., 1998; Li and Heap, 2014; Tabios III and Salas, 1985; Wagner et al., 2012; Zhang and Srinivasan, 2009). Generally speaking, interpolation schemes that use covariates (e.g. elevation) are preferable (Wagner et al., 2012). Stochastic methods such are kriging, are usually more accurate than simpler deterministic approaches such as inverse distance weighting (Tabios III and Salas, 1985). However, differences may be small and other criteria such as ease of parameterization and computational efficiency are also important to drive methodological choices (Dirks et al., 1998; Thornton et al., 1997). Package meteoland implements, with a few modifications, the daily weather interpolation and estimation algorithms that underpin the U.S. DAYMET dataset (https://daymet.ornl.gov/) (Thornton et al., 1997; Thornton and Running, 1999). This approach, similar to inverse distance weighting, interpolates weather variables using truncated Gaussian filters, which consist in defining spatial weights $W(r)$ at radial distance r from a target point p using:

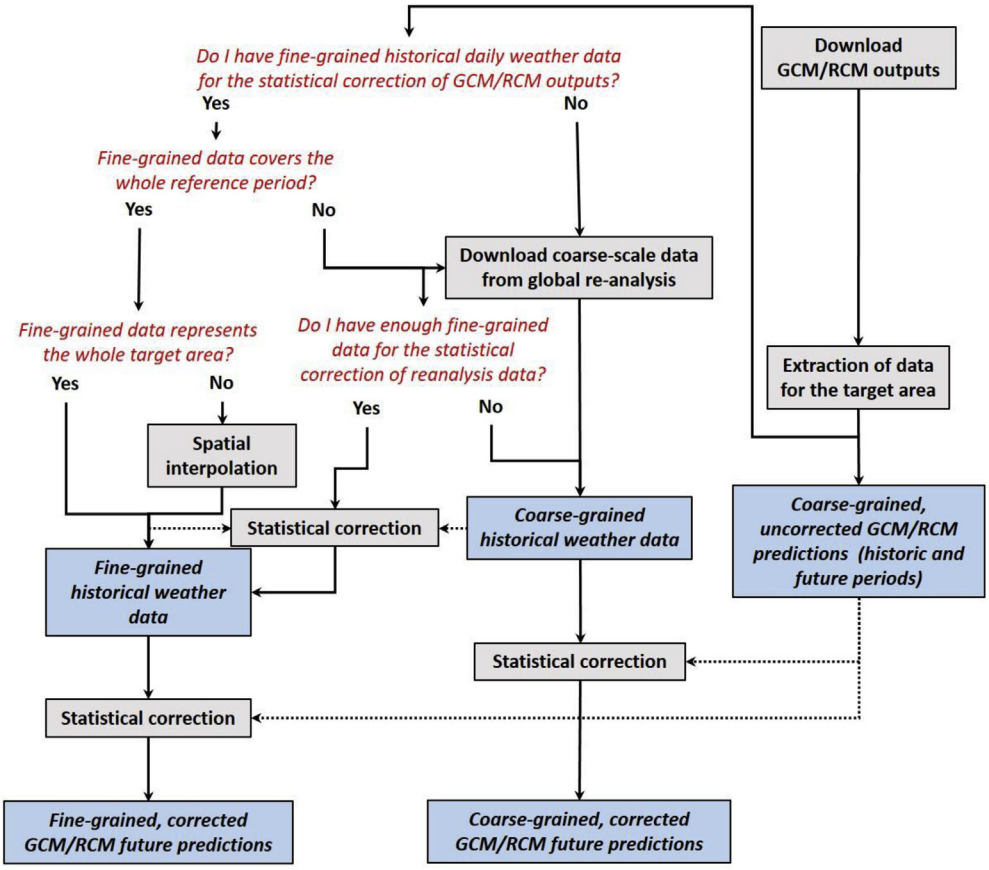
Do I have fine-grained historical daily weather data for the statistical correction of GCM/RCM outputs?
Yes
No
Fine-grained data covers the whole reference period?
Yes
No
Download coarse-scale data from global re-analysis
Fine-grained data represents the whole target area?
Yes
No
Do I have enough fine-grained data for the statistical correction of reanalysis data?
Yes
No
Spatial interpolation
Statistical correction
Coarse-grained historical weather data
Fine-grained historical weather data
Statistical correction
Statistical correction
Fine-grained, corrected GCM/RCM future predictions
Coarse-grained, corrected GCM/RCM future predictions
Download GCM/RCM outputs
Extraction of data for the target area
Coarse-grained, uncorrected GCM/RCM predictions (historic and future periods)

Fig. 1. Example of workflow to obtain corrected climate model (GCM or RCM) future predictions of daily weather for a given target area. Questions are indicated in red, tasks are indicated in gray boxes and data in blue boxes. Continuous-line arrows represent work flows and dotted arrows represent the use of data in tasks. (For interpretation of the references to colour in this figure legend, the reader is referred to the Web version of this article.)

$$W(r) = \begin{cases} e^{-\alpha(r/R_p)^2} - e^{-\alpha} & \text{if } r \le R_p \\ 0 & \text{otherwise} \end{cases} \quad (1)$$

where R_p is the truncation distance and α is a kernel shape parameter. For each target point, the spatial convolution of this filter with a set of weather stations results in a vector of weights. R_p is automatically adjusted so that it is smaller in data-rich regions and is increased in data-poor regions. The estimation of R_p is based on N, the average number of observations to be included for each target point, and is done using the following algorithm (Thornton et al., 1997):

1. A user-specified value is used to initialize R_p.
2. Interpolation weights W_i are calculated (eq. (1)) for all $i = (1, \ldots, n)$ stations, and the local station density is calculated as:

$$D_p = \frac{\sum_{i=1}^{n} (W_i / \overline{W})}{R_p^2 \cdot \pi} \quad (2)$$

where $\overline{W}$ is the average weight over the untruncated region of the filter, calculated as:

$$\overline{W} = \left(\frac{1 - e^{-\alpha}}{\alpha} \right) - e^{-\alpha} \quad (3)$$

3. A new R_p value is calculated as a function of N and D_p, as:

$$R_p = \sqrt{\frac{N*}{D_p \cdot \pi}} \quad (4)$$

where $N^* = 2N$ for the first $I - 1$ iterations, and $N^* = N$ for the final iteration.

Table 1
Overview of the main functions in meteoland.

Function(s)	Description
correctionpoints	Statistical correction of weather data series
correctionpoints.errors	Evaluation of errors before and after statistical correction
downloadAEMEThistorical/downloadAEMETcurrentday	Download data from the Spanish National Meterology Agency
extractNetCDF	Extract RCM output from NetCDF files
extractgridpoints/extractpointdates	Extract/reshape weather data from/to R objects
interpolationpoints/interpolationpixels/interpolationgrid	Interpolation and estimation of weather from station data
interpolation.calibration/interpolation.cv	Calibration and cross-validation of interpolation procedures
interpolation.coverage	Analyze spatial and temporal coverage of interpolation data
meteoplot	Plot a weather data series at the desired temporal resolution
penman	Penman's reference evapotranspiration (McMahon et al., 2013)
precipitationconcentration	Daily precipitation concentration index (Martin-Vide, 2004)
readmeteorologypointfiles/writemeteorologypointfiles	Read/write point weather data series from/to the disk
readmeteorologygridfiles/writemeteorologygridfiles	Read/write weather data of full spatial grids from/to the disk
readmeteorologypixelsfiles/writemeteorologypixelsfiles	Read/write weather data of a subset of grid cells from/to the disk
summarypoints/summarygrid/summarypixels	Summarize (temporally) the series of a weather variable

4. The new R_p value is substituted in step (2) and steps (2–4) are iterated a specified number of times I. The final R_p value is used to calculate the final interpolation weights.

In meteoland estimation of R_p is done once for each target point, variable and day. Interpolation of temperature includes a correction for the effects of elevation. More specifically, a weighted least-squares regression is used to assess the relationship between temperature differences and elevation differences in weather station data and this relationship is applied to elevation differences between weather stations and the target point (Thornton et al., 1997). Interpolation of relative humidity is done after transforming it to dew-point temperature (Liston and Elder, 2006). No correction for elevation is performed during interpolation, but elevation effects arise when back-transforming dew-point temperature to relative humidity. Interpolation of daily precipitation is complicated by the need to predict both precipitation occurrence and, conditioned on this, precipitation amount. Thornton et al. (1997) defined a binomial predictor of spatial precipitation occurrence as a function of the weighted occurrence at surrounding weather stations. Conditional on precipitation occurrence, the interpolation routine predicts precipitation amount, where weighted least-squares regression is also used to account for elevation effects. Interpolation of wind is performed in three different ways depending on the information available. If only wind speed data is available, the spatial interpolation with Gaussian weights is used on wind scalars as described above. If weather station data includes wind direction, a polar average is calculated using Gaussian weights. Finally, if static wind fields are also available (e.g., Forthofer et al., 2014) the interpolation routine first finds, for each weather station the wind field that best matches the observed vector. Then, the wind vectors extracted from the selected wind fields are averaged as before. Details of the interpolation of each variable can be found in the R package vignette.

Daily potential solar radiation, R_{pot}, is estimated from solar constant, solar declination, latitude, aspect and slope according to Garnier and Ohmura (1968). Instantaneous potential radiation $R_{pot,s}$ is calculated using:

$$\begin{aligned} t_1 &= -\sin\varphi\cdot\cos H\cdot\cos A\cdot\sin Z_x - \sin H\cdot\sin A\cdot\sin Z_x \\ &\quad + \cos\varphi\cdot\cos H\cdot\cos Z_x \\ t_2 &= \cos\varphi\cdot\cos A\cdot\cos Z_x + \sin\varphi\cdot\cos Z_x \\ R_{pot,s} &= I_0\cdot[t_1\cdot\cos\delta + t_2\cdot\sin\delta] \end{aligned} \quad (5)$$

where ϕ is latitude, H is the hour angle measured from solar noon, A is aspect measured from north, Z_x is the angle of slope, δ is solar declination and I_0 is the solar constant. Daily potential radiation is obtained by integrating $R_{pot,s}$ between sunrise and sunset. Incident solar radiation, R_g, the amount of solar radiation reaching a surface after accounting for the atmosphere, is then calculated as (Thornton and Running, 1999):

$$R_g = R_{pot}\cdot T_{t,max}\cdot T_{f,max} \quad (6)$$

where $T_{t,\max}$ is the daily-average (i.e. between sunrise and sunset) maximum (cloud-free) total transmittance and $T_{f,\max}$ is the proportion of $T_{t,\max}$ realized on a given day (i.e. cloud correction). $T_{t,\max}$ and $T_{f,\max}$ are calculated using the interpolated estimates of temperature, relative humidity and precipitation (Thornton and Running, 1999). The package provides additional functions to divide daily incident radiation into (sub-daily) instantaneous estimates of direct and diffuse radiation (Spitters et al., 1986).

2.3. Statistical correction

Generally speaking, the statistical correction of a weather data series using a more accurate series is necessary when the more accurate series does not cover the period of interest and the less accurate one does. In principle, both series can be at the same spatial scale, but most often the less accurate series will be at broader scale. When used for downscaling coarse-scale reanalysis data, statistical corrections can be broadly referred to as 'empirical-statistical downscaling' (Benestad et al., 2008). When applied to post-processing climate model outputs, this kind of downscaling usually implies an attempt to correct model biases and is often termed 'empirical-statistical downscaling and error correction' (Themeβl et al., 2012). Although there are many ways to perform statistical corrections, meteoland currently offers three options:

- 'Unbiasing': consists in subtracting, from the series to be corrected, the average difference between the two series for the reference period (Déqué, 2007). Let x_i be the value of the variable of the more accurate (e.g., local) series for a given day i and u_i the corresponding value for the less accurate series (e.g., climate model output). The bias, θ, is the average difference over all n days of the reference period:

$$\theta = \sum_i^n (u_i - x_i)/n = \sum_i^n u_i/n - \sum_i^n x_i/n \quad (7)$$

The bias calculated in the reference period is then subtracted from the value of u for any day of the period of interest.

- 'Scaling': A slope is calculated by regressing u on x through the origin (i.e. zero intercept) using data of the reference period. The slope can then be used as scaling factor to multiply the values of u for any day of the period of interest. This method should be preferred to 'unbiasing' for non-negative variables (e.g. wind speed).
- 'Empirical quantile mapping': Due to its distributional properties, neither multiplicative or additive factors are appropriate for daily precipitation (Gudmundsson et al., 2012; Ruffault et al., 2014). In this case it has been recommended to compare the empirical cumulative distribution function (CDF) of the two series for the reference period (Gudmundsson et al., 2012; Themeβl et al., 2011). The empirical CDFs of x and u for the reference period are approximated using tables of empirical percentiles, and this mapping is used to correct values of u for the period of interest:

$$c_d = ecdf_x^{-1}(ecdf_u(u_d)) \quad (8)$$

where $ecdf_x$ and $ecdf_u$ are the empirical CDFs of x and u, respectively. Values between the percentiles are approximated using linear interpolation. meteoland performs quantile mapping by calling functions from R package qmap (Gudmundsson, 2016).

For each target location to be processed, the correction routine first determines which is the nearest climate model cell and extracts its weather data series for the reference period and the period of interest. Statistical corrections are done for each of the twelve months separately to account for seasonal variation of distributional differences (Ruffault et al., 2014). Although users can choose their preferred correction method for each variable, *meteoland* has default approaches. The unbiasing method is used to correct values of mean temperature and radiation, whereas precipitation values are by default corrected using empirical quantile mapping, including a correction for the frequency of wet days. To correct minimum (respectively maximum) temperature values, scaling is applied to the difference between minimum (resp. maximum) temperature and mean temperature. Scaling is also applied to wind speed. Mean relative humidity is first transformed to specific humidity, the unbiasing method is applied to this variable and the result is back transformed to mean, minimum and maximum relative humidity using the previously corrected series of mean, maximum and minimum temperature, respectively.

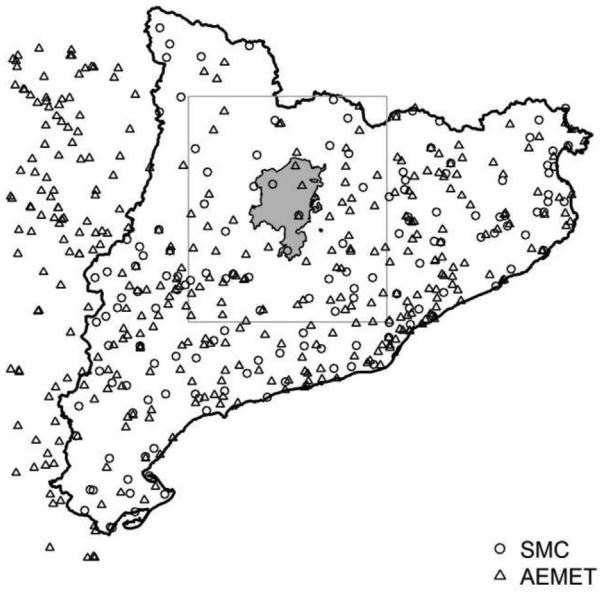

Fig. 2. Location of weather stations from the Catalan Meteorological Service (SMC) and the Spanish Meteorological Agency (AEMET) networks with data for year 2001 in Catalonia and neighboring areas. Solsonès county is shaded and the gray box indicates the boundaries of the subset of weather stations used for interpolation within the county.

3. Examples of application

3.1. Calibration and validation of weather interpolation in Catalonia

We compiled year 2001 meteorology data of 506 stations within and around the region of Catalonia (NE of Spain) (Fig. 2), from the Catalan Meteorological Service and the Spanish Meteorological Agency (Tomas-Burguera et al., 2016).

Interpolation parameters α and N were calibrated for minimum temperature, maximum temperature, dew-point temperature and precipitation. Using function 'interpolation.calibration', we determined for each variable the pair of parameter values corresponding to a minimum mean absolute error (MAE). For minimum and maximum temperature, MAE was smaller when both N and α increased simultaneously, and optimum values were $N_{opt,\ Tmax} = N_{opt,\ Tmin} = 60$ and $\alpha_{opt,Tmax} = \alpha_{opt,Tmin} = 9.5$ (Table A1 and Fig. A1 in Appendix A). Optimum interpolation of dew-point temperature implied weights estimated using fewer points ($N_{opt,\ Tdew} = 10$; $\alpha_{opt,Tdew} = 2.5$). We calibrated interpolation parameters for precipitation in two steps, using cost functions that accounted for errors in the spatial and temporal patterns. First, we determined the parameter combination for interpolation occurrence weights resulting in a minimum value of the geometric average between the *MAE in the frequency of rainy days* and the *MAE in the frequency of rainy stations*. Optimum values corresponded to $N_{opt,\ Pocc} = 5$ and $\alpha_{opt,Pocc} = 10$, meaning that the occurrence of precipitation in a small set of stations close to the target point was often sufficient to predict precipitation events. Given these optimum parameters for occurrence, we then determined the parameter combination for interpolation precipitation amount weights resulting in a minimum value of the geometric average between the *MAE in the average daily precipitation* and the *MAE in the average station precipitation*. The precipitation patterns of a larger area ($N_{opt,Pam} = 60$ and $\alpha_{opt,Pam} = 1$), were needed to ensure the reliability of regression coefficients (Fig. A2).

Using the optimum interpolation parameters and function interpolation.cv, we conducted an evaluation of the prediction errors for all meteorological variables except wind by leave-one-out cross validation. As performance statistics we used MAE, bias and Pearson's correlation coefficient. MAEs for daily predicted vs. observed minimum and maximum temperatures were 1.5 °C and 1.4 °C respectively. Bias for minimum temperature was negligible (+0.00029 °C), but a small positive bias was found for maximum daily temperature (+0.12 °C). Observed and predicted distributions of both variables were very similar except at the extremes (Fig. A3). Predictions of temperature range had slightly higher errors and the predicted distribution underrepresented extreme values (Table 2; Fig. A3). Of all station-days with precipitation data, the interpolation procedure predicted 19.6% wet days, very close to observed 19.5% wet days. Success rate for occurrence of precipitation was 87.4% (92.1% for dry days and 68.0% for wet days). MAE for annual precipitation (across stations) was 67.7 mm, with errors being larger for stations with larger annual precipitation (Fig. A4). Observed and predicted distributions of precipitation values were very similar for values up to 150 mm and the predicted frequency of daily wet stations closely matched the observed frequency (Fig. A4). MAE for relative humidity was 6.9% and bias was 0.04%, with predicted distribution underrepresenting low humidity values (Fig. A5). Cross-validation MAEs for radiation was 2.5 MJ m^{-2} and bias was −0.02 MJ m^{-2}, with very low and very high radiation values being slightly underrepresented (Fig. A.6).

3.2. Weather interpolation over Solsonès county

We used function 'interpolationpixels' to interpolate daily meteorology for year 2001 and over 100,073 cells of 1 ha covering Solsonès (1001 km^2), a county in the central part of Catalonia (Fig. 1). The county has complex topography, including an elevation gradient from south to north (Fig. 3; first row). Using a buffer of 30 km around the county, 63 weather stations had temperature data, 79 stations had precipitation data, 29 stations had relative humidity data and only 19 stations had wind speed data. Fig. 3 shows the result of estimating meteorology for a particular day (2001-03-01; second and third row)

Table 2
Validation statistics: n – number of station-days; r – linear correlation coefficient; *MAE* – mean absolute error; $SD_{stations}/SD_{days}$ – standard deviation of MAE across stations/days. 'Date rainfall' is the sum of precipitation across stations for each date and 'Date precipitation stations' is the number of stations with precipitation events for each date.

			MAE			Bias		
Variable	n	r	Value	$SD_{stations}$	SD_{days}	Value	$SD_{stations}$	SD_{days}
Minimum temperature (°C)	124,339	0.96	1.50	0.84	0.22	0.00	1.45	0.07
Maximum temperature (°C)	124,216	0.96	1.44	1.40	0.16	0.12	1.80	0.07
Temperature range (°C)	124,018	0.77	1.97	1.13	0.28	0.12	1.91	0.07
Relative humidity (%)	55,430	0.80	6.85	4.02	0.91	0.04	7.12	0.76
Radiation (MJ·m^{-2})	44,900	0.92	2.53	0.46	1.10	−0.02	1.03	1.94
Station annual rainfall (mm· yr^{-1})	501	0.90	67.7	77.9		0.03	103.2	
Station precipitation days	501	0.33	20.8	19.3		0.45	28.4	
Date rainfall (mm)	357	0.99	29.4		51.0	0.06		58.9
Date precipitation stations	357	0.99	3.77		3.63	0.65		5.20

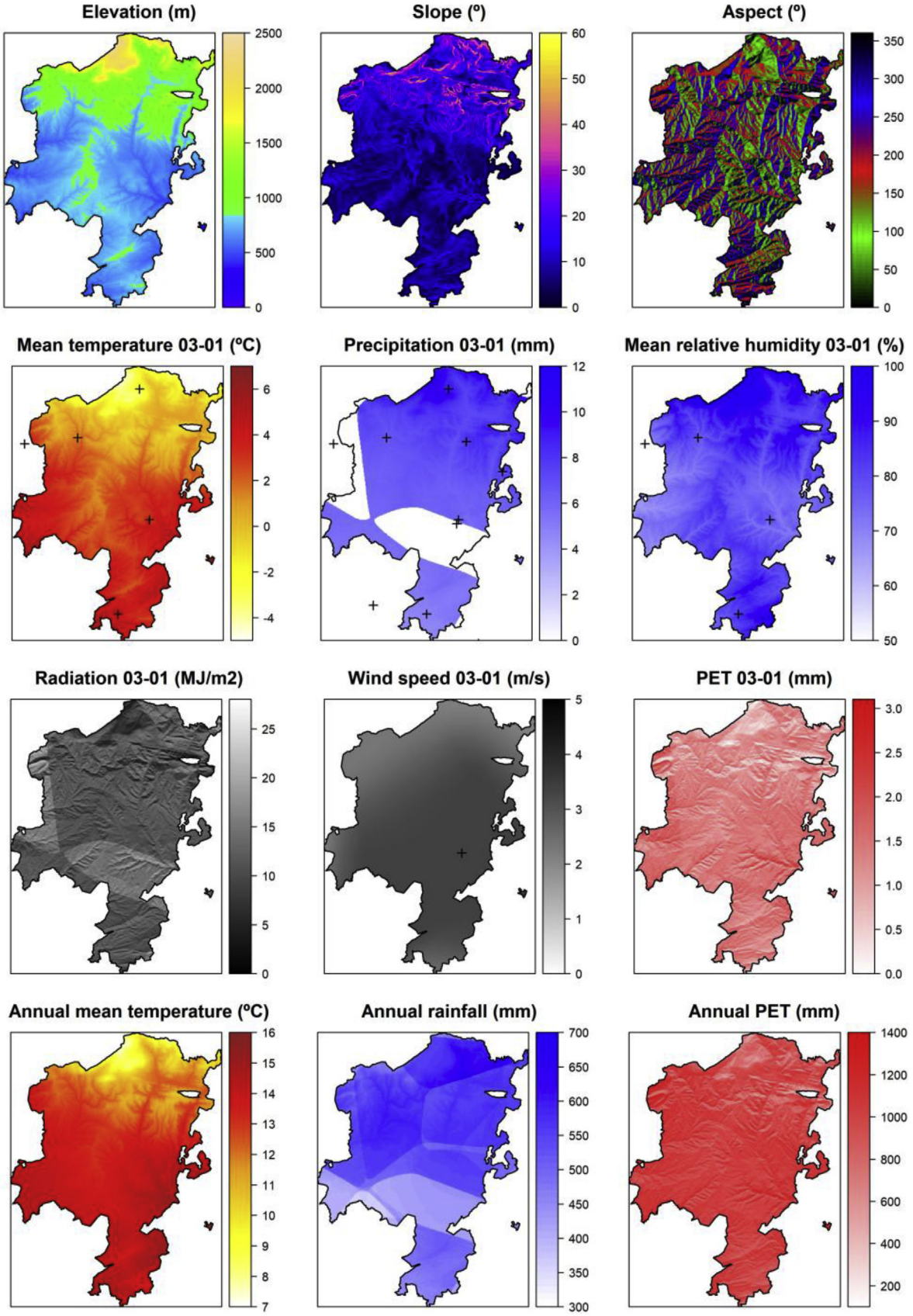

Fig. 3. Topography (first row) and weather interpolation over Solsonès county (daily results in second and third rows, and annual summaries in the fourth row).

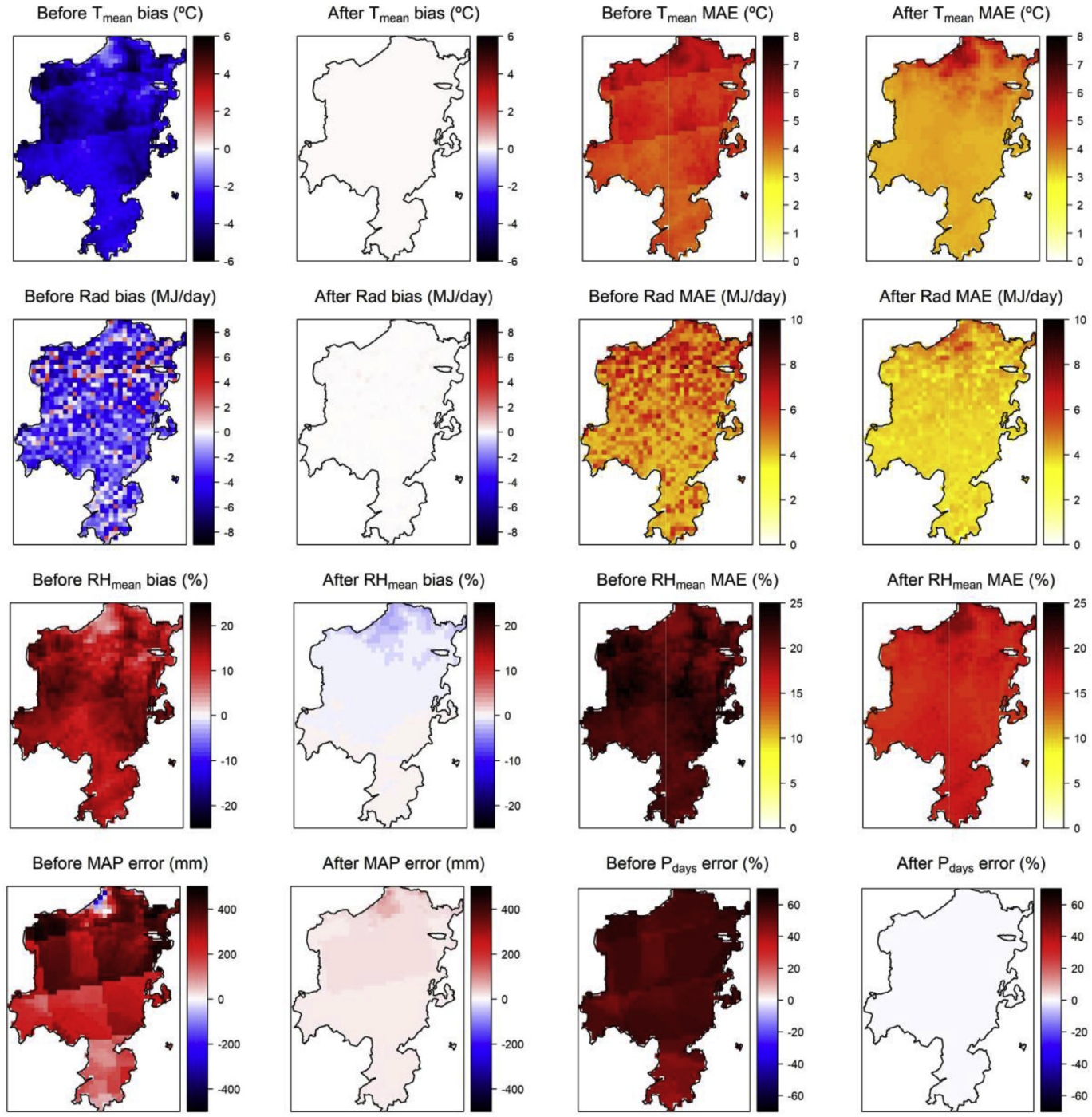
Before T_{mean} bias (ºC)
After T_{mean} bias (ºC)
Before T_{mean} MAE (ºC)
After T_{mean} MAE (ºC)
Before Rad bias (MJ/day)
After Rad bias (MJ/day)
Before Rad MAE (MJ/day)
After Rad MAE (MJ/day)
Before RH_{mean} bias (%)
After RH_{mean} bias (%)
Before RH_{mean} MAE (%)
After RH_{mean} MAE (%)
Before MAP error (mm)
After MAP error (mm)
Before P_{days} error (%)
After P_{days} error (%)

Fig. 4. Comparison between RCM (CCLM4-8-17 driven by CNRM-CERFACS-CNRM-CM5) and interpolated daily data for the historical period (1976–2005), before and after statistical correction. Bias and mean absolute error (MAE) are shown in the first three rows for mean temperature (T_{mean}), radiation (Rad) and mean relative humidity (RH_{mean}). The fourth row shows the error in mean annual precipitation (MAP) and in the number of days with precipitation (P_{days}), before and after corrections.

and the 2001 annual statistics (last row). Influence of elevation was clear on interpolated daily patterns for temperature and relative humidity. Estimated radiation was strongly determined by aspect and slope, but was also influenced by precipitation events, with no precipitation areas receiving more radiation. Wind speed had the simplest spatial structure because wind data was scarce. After averaging daily maps, mean annual temperature (MAT) and mean annual precipitation (MAP) also reflected topographic influences, although tessellation of rainfall patterns aroused following the location of stations.

3.3. Downscaling/correcting climate model predictions for the Solsonès county

We now illustrate the usage of *meteoland* for downscaling and correcting climate model predictions over Solsonès county. Daily weather predictions of the CNRM-CERFACS-CNRM-CM5 global model, downscaled to Europe at 11 km resolution by the CCLM4-8-17 regional climate model (RCM), were obtained for the historical period 1976–2005 and the projection period 2006–2100 (under Representative Concentration Pathway, RCP, 8.5) from the EU-CORDEX project

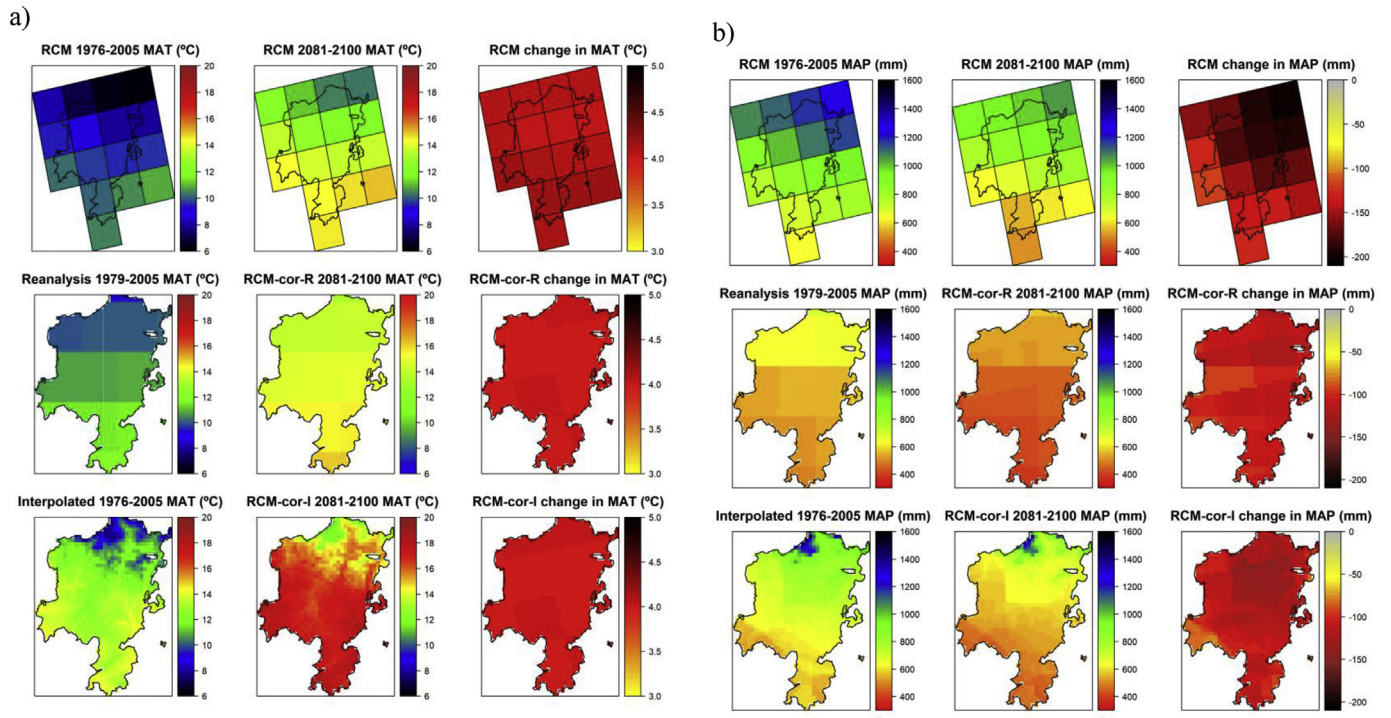
a)
RCM 1976-2005 MAT (ºC)
RCM 2081-2100 MAT (ºC)
RCM change in MAT (ºC)
Reanalysis 1979-2005 MAT (ºC)
RCM-cor-R 2081-2100 MAT (ºC)
RCM-cor-R change in MAT (ºC)
Interpolated 1976-2005 MAT (ºC)
RCM-cor-I 2081-2100 MAT (ºC)
RCM-cor-I change in MAT (ºC)
b)
RCM 1976-2005 MAP (mm)
RCM 2081-2100 MAP (mm)
RCM change in MAP (mm)
Reanalysis 1979-2005 MAP (mm)
RCM-cor-R 2081-2100 MAP (mm)
RCM-cor-R change in MAP (mm)
Interpolated 1976-2005 MAP (mm)
RCM-cor-I 2081-2100 MAP (mm)
RCM-cor-I change in MAP (mm)

Fig. 5. Statistical downscaling and correction of RCM predictions (CCLM4-8-17 driven by CNRM-CERFACS-CNRM-CM5 under RCP 8.5) for temperature (a) and precipitation (b) across Solsonès. First panels show, on RCM 11-km cells, the mean annual temperature (MAT) or mean annual precipitation (MAP) for the reference period (1976–2005), for the projected period (2081–2100) and the difference between the two. Second row panels show the same annual statistics for ERA-interim data (0.125° resolution) and the reference period, the projected period after correcting RCM predictions and the difference between the two. Third row panels show the same statistics as panels in the second row, but using weather station data interpolated at 1 km as reference.

(Kotlarski et al., 2014), available at the Earth System Grid Federation (http://esgf.llnl.gov/). We used the function 'extractNetCDF' to subset the RCM predictions corresponding to the Solsonès county. To obtain reference historical series on each of 998 1-km grid cells over Solsonès, we used either: (a) ERA-interim daily re-analysis data (1979–2005) at 0.125° resolution (original grid at 0.5° resolution) (Dee et al., 2011), available at https://software.ecmwf.int/; or (b) interpolated weather data (1976–2005) at 1 km resolution, obtained using 'interpolationpoints' and weather station data from the previous examples.

We used function 'correctionpoints.errors' with interpolated data as reference to evaluate the errors of RCM predictions before and after statistical correction. Before correction, there was a negative bias in mean temperature and radiation; and a positive bias in mean relative humidity (Fig. 4). Correction methods were kept to variable defaults, and errors after correction were determined by cross-validation (i.e., by removing 1 month at a time from the historical period). Correction of RCM predictions nearly eliminated biases in the previous three variables, but small negative biases remained in relative humidity for high-elevation areas (Fig. 4). MAE values were also substantially lower after correction, being residual MAE larger at high elevations. Before correction, mean annual precipitation (MAP) predicted by the RCM was substantially larger than observed (average + 280 mm) and the proportion of days with precipitation were also over-predicted (average + 55%), probably caused by "drizzle" effect (Fig. 4). Errors in MAP and in the proportion of days with precipitation were strongly reduced after correction.

We used function 'correctionpoints' to correct RCM projections (2006–2100) on each 1-km grid cell, using either reanalysis data or interpolated data as historical reference. As before, default correction methods were applied. Large differences existed in patterns of mean annual temperature (MAT) between RCM outputs, reanalysis data and interpolated data for the historical period, and these differences persisted after correction for the projected period (Fig. 5a). However, temperature correction did not substantially alter the 4 °C MAT increase predicted for RCP 8.5. This was not the case for mean annual precipitation (MAP). Not only the uncorrected RCM outputs generally overestimated MAP, compared to reanalysis and interpolated data, but also the projected decrease in MAP was milder after corrections: an average 160 mm reduction for uncorrected RCM data vs. 107 mm and 116 mm for correction with reanalysis data and interpolated data, respectively (Fig. 5b). This difference in the predicted MAP trend is the result of the non-linear transformation of trends obtained by empirical quantile mapping (Maraun et al., 2017b).

3.4. Evaluation of the effect of climate change corrections on forest drought

We applied the water balance model of De Cáceres et al. (2015) to 573 forest plots in the Solsonès county to illustrate how the predicted impacts of climate change on forest drought may be affected by the correction and downscaling of RCM outputs. The purpose of the model is to predict daily variations in soil water content and assess drought stress for woody plants within forest stands. Forest plot data was obtained from the Third Spanish Forest Inventory (Villanueva, 2004). For simplicity, forest structure and composition was assumed constant during simulations; and soil was assumed to be 1 m deep, divided into two layers (0–30 cm; 30–100 cm). Parameter values for species (e.g., leaf area, canopy storage capacity, light extinction coefficient) and soil attributes (e.g., texture, rock fragment content, macroporosity) were set as detailed in De Cáceres et al. (2015). For each forest plot, we simulated daily water balance for two 20-yr periods within the 21st century (2006–2025 and 2081–2100) and using three meteorological inputs: (a) the uncorrected climate series of the corresponding RCM cell; (b) the corrected climate series obtained using correctionpoints and ERA-interim data (0.125° resolution) as reference; and (c) the corrected climate series obtained using correctionpoints and interpolated weather station data (1 km resolution) as reference. For all plants in a forest plot,

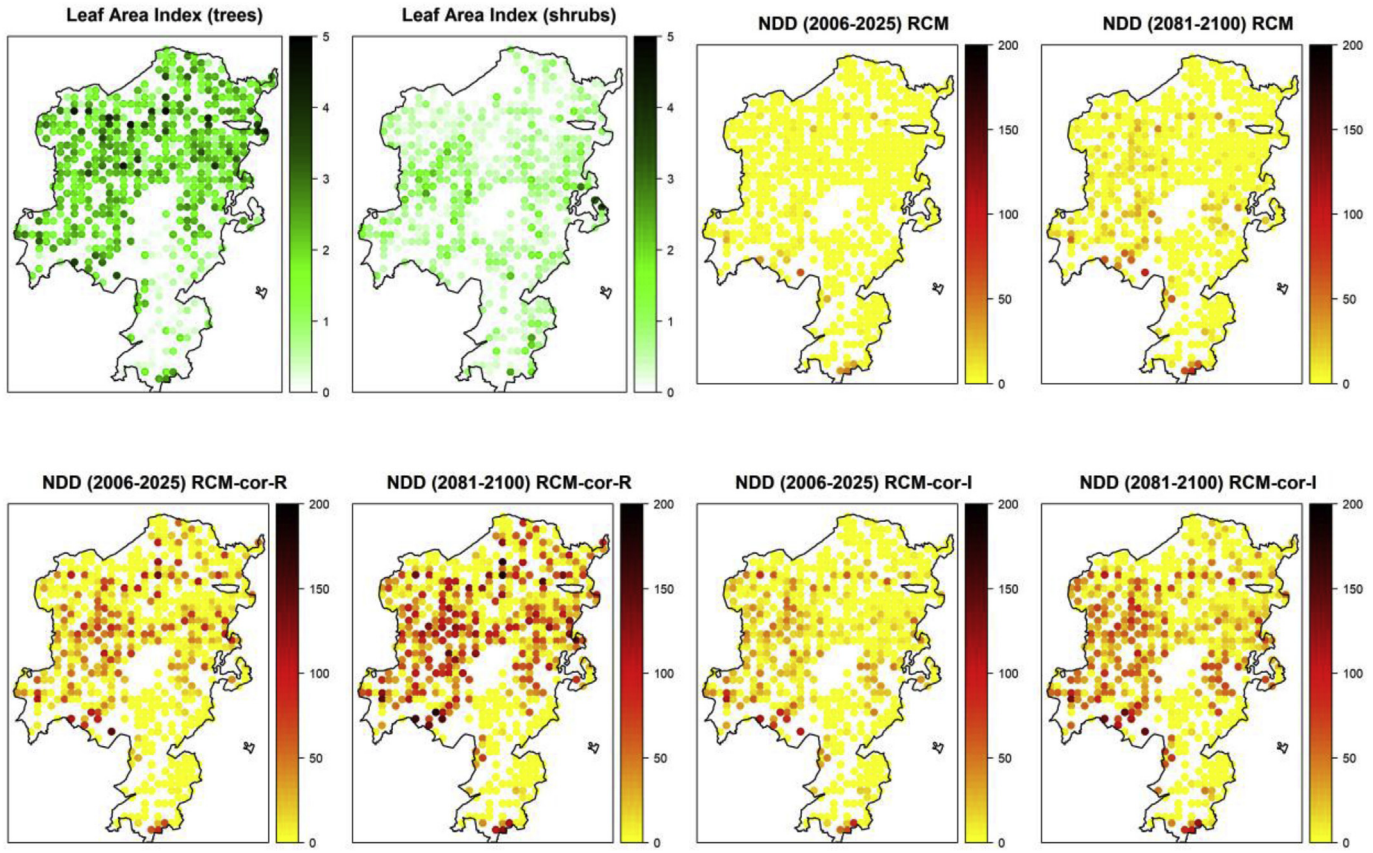

Fig. 6. Leaf area index (m^2/m^2) of trees and shrubs of forest plots (upper row); and average annual number of consecutive drought days (NDD) as simulated by the water balance model for the 2006–2025 and 2081–2100 periods and using RCM predictions (CCLM4-8-17 driven by CNRM-CERFACS-CNRM-CM5 under RCP 8.5) without correction (RCM) and after applying statistical correction using either re-analysis data (RCM-cor-R) or interpolated data (RCM-cor-I) as reference.

the water balance model produces daily drought stress values, scaled between 0 and 1 and calculated as the one-complement of whole-plant relative conductance. As indication of annual drought duration in each plot, we calculated the maximum number of consecutive days where the average drought stress of the plot was larger than 0.5 (De Cáceres et al., 2015; Mouillot et al., 2002). Values of annual drought duration were averaged for each plot, simulated period and meteorological input.

Regardless of the simulated period, the number of drought days (NDD) was often small when RCM projections were not corrected (Fig. 6). While this result contrasts with the strong reduction in MAP predicted by uncorrected RCM projections (Fig. 5b), it may be explained by historical biases of uncorrected RCM data (positive bias in MAP and relative humidity; negative bias in radiation and temperature; Fig. 4). These biases led the water balance model to unrealistically underestimate drought stress in the target area for both periods. Corrections conducted using reanalysis data led to a much higher frequency of drought days compared to the uncorrected data (Fig. 6). Nevertheless, they were still not satisfactory, because of the strong water deficits predicted in northwest mountainous areas under current and future conditions, resulting from a poor representation of altitudinal precipitation gradients (Fig. 5b). When applying corrections with fine resolution (interpolated) data, increases in NDD between the two simulated periods (2006–2025 and 2081–2100) were found to be largest in plots of the western areas. Southern areas did not obtain such increases, despite having a drier climate, because of plots having low values of leaf area (Fig. 6). Northwest mountain forests were not predicted to be strongly affected by drought impacts, despite their high leaf area and the predicted decrease in precipitation, indicating that precipitation by the end of the century was still sufficient to avoid forest drought stress.

4. Remarks, limitations and potential improvements

In our opinion the greatest value of the package presented here is that it offers an integrated and easy-to-use platform to perform the full chain of tasks required to obtain consistent daily weather data at fine spatial resolution for current and future conditions (e.g. Fig. 1). With the aim to reduce the burden on the user side, the package offers a limited set of statistical options with default parameterizations. While we initially designed *meteoland* to provide suitable inputs for modelling climate change impacts on forests, we believe it may be useful for any kind of research studies requiring fine grained climatic data (e.g. agronomy, hydrology, ecology, forestry, …). Calibration and, especially, validation of interpolation routines should be conducted for each weather station data set and target period. Similarly, an evaluation of residual errors is recommended for the historical simulations of every climate model, before using the package to correct its projections (but see Maraun et al., 2017b).

Despite its advantages, we are aware that the algorithms currently implemented in *meteoland* may not be optimal for all situations, and future work should be directed to improve current methods or even complement them with others. As the philosophy of *meteoland* is to discharge the end user from performing extensive literature reviews and comparisons of available methods, we plan on undergoing these tasks ourselves and, when necessary, implement new routines or wrappers to call functions of other packages. In the case of bias correction, the largest disadvantage of the methods currently offered is that they ignore the dependency between weather variables, although this issue may be less critical when correcting high-resolution climate

model outputs (Hempel et al., 2013). Moreover, the advantages/disadvantages of alternative forms of bias correction, including the role of cross-validation, are still being discussed (Ehret et al., 2012; Gobiet et al., 2015; Maraun et al., 2017b; Themeβl et al., 2012). While climatologists usually prefer having as many options as possible for method comparison and testing, we envision *meteoland* as a platform where an informed subset of all the available methods is offered to the climate-driven impact researcher. This implies that the development of the package should involve collaborative work between climatologists and climate-impact researchers, who should be guided to fast and robust methods, but not necessarily the most accurate or sophisticated ones. The package should offer several choices only when the alternative to be advised depends on factors that the end user is able to easily identify.

Besides revising the methods currently offered for interpolation and statistical correction, other aspects of the package could be improved to facilitate climate-driven impact studies. The calculation of insolation could be improved by taking into account shading from nearby topographic elements, for example by calling functions of package *RSAGA* (Brenning, 2008). The data structures of *meteoland* have been designed to store daily data, but they could be generalized to store data at other temporal scales (e.g., sub-daily). The package currently offers the possibility to access public weather data from the Spanish National Meteorological Agency, but similar routines could be added to access observations, forecasts or reanalysis data from other providers if the necessary programming interfaces are available (Iannone, 2015). The package could also be improved by incorporating weather generation tools (Cordano and Eccel, 2016), which would allow considering the uncertainty in the daily series obtained after downscaling/correction of climate model outputs. Finally, although the package is already quite fast (most routines are implemented in C++), computation speed could be increased through parallelization.

Author's contributions

MDC conceived the design of the package and implemented most functions. NMS, VG and AC contributed their code to specific functions and package features. All authors participated in the design and interpretation of illustrative examples and contributed to manuscript writing.

Software availability

Package 'meteoland' is freely available at CRAN (https://CRAN.R-project.org/package=meteoland) and detailed information on how to use it can be found at the package website: http://vegmod.ctfc.cat/meteolandweb. Development versions can be found at http://github.com/miquelcaceres/meteoland

Acknowledgements

We thank the 'Agencia Estatal de Meteorología (AEMET)' and 'Servei Meteorològic de Catalunya' (SMC) for providing daily weather station data. Authors are grateful to Marc Stéphanon, Sergio Vicente-Serrano and three anonymous reviewers for insightful comments on previous versions of this manuscript. This work was supported by the ERA-Net FORESTERRA project INFORMED (PCIN-2014-050), by project CGL2014-59742-C2-2-R (Spanish Ministry of Economy and Competitiveness), by a Spanish "Ramon y Cajal" fellowship to M.D.C (RYC-2012-11109) and by a Spanish "Juan de la Cierva" fellowship to M.T. (IJCI-2015-26953).

Appendix A. Supplementary data

Supplementary data related to this article can be found at https://doi.org/10.1016/j.envsoft.2018.08.003.

References

Bedia, J., Gutierrez, J.M., Herrera, S., Iturbide, M., Manzanas, R., 2015. downscaleR: an R Package for Bias Correction and Statistical Downscaling. R package version 2.0.4.
Bedia, J., Herrera, S., Gutiérrez, J.M., 2013. Dangers of using global bioclimatic datasets for ecological niche modeling. Limitations for future climate projections. Global Planet. Change 107, 1–12. https://doi.org/10.1016/j.gloplacha.2013.04.005.
Benestad, R.E., Chen, D., Hanssen-bauer, I., 2008. Empirical Statistical Downscaling. World Scientific Publishing Company, New Jersey. https://doi.org/10.1142/6908.
Benestad, R.E., Mezghani, A., Parding, K.M., 2017. Esd: Climate Analysis and Empirical-statistical Downscaling (ESD) Package for Monthly and Daily Data. R package version 1.7918.
Brenning, A., 2008. Statistical geocomputing combining R and SAGA: the example of landslide susceptibility analysis with generalized additive models. In: In: Boehner, J., Blaschke, T., Montanarella, L. (Eds.), SAGA - Seconds Out (= Hamburger Beitraege Zur Physischen Geographie Und Landschaftsoekologie, vol. 19. pp. 23–32.
Christensen, J.H., Boberg, F., Christensen, O.B., Lucas-Picher, P., 2008. On the need for bias correction of regional climate change projections of temperature and precipitation. Geophys. Res. Lett. 35. https://doi.org/10.1029/2008GL035694.
Cordano, E., Eccel, E., 2016. Tools for stochastic weather series generation in R environment. Ital. J. Agrometeorol. 21, 31–42. https://doi.org/10.19199/2016.3.2038-5625.031.
Daly, C., Gibson, W.P., Taylor, G.H., Johnson, G.L., Pasteris, P., 2002. A knowledge-based approach to the statistical mapping of climate. Clim. Res. 22, 99–113. https://doi.org/10.3354/cr022099.
Davi, H., Dufrêne, E., Francois, C., Le Maire, G., Loustau, D., Bosc, a., Rambal, S., Granier, a., Moors, E., 2006. Sensitivity of water and carbon fluxes to climate changes from 1960 to 2100 in European forest ecosystems. Agric. For. Meteorol. 141, 35–56. https://doi.org/10.1016/j.agrformet.2006.09.003.
De Cáceres, M., Martínez-Vilalta, J., Coll, L., Llorens, P., Casals, P., Poyatos, R., Pausas, J.G., Brotons, L., 2015. Coupling a water balance model with forest inventory data to predict drought stress: the role of forest structural changes vs. climate changes. Agric. For. Meteorol. 213, 77–90. https://doi.org/10.1016/j.agrformet.2015.06.012.
Dee, D.P., Uppala, S.M., Simmons, A.J., Berrisford, P., Poli, P., Kobayashi, S., Andrae, U., Balmaseda, M.A., Balsamo, G., Bauer, P., Bechtold, P., Beljaars, A.C.M., van de Berg, L., Bidlot, J., Bormann, N., Delsol, C., Dragani, R., Fuentes, M., Geer, A.J., Haimberger, L., Healy, S.B., Hersbach, H., Hólm, E.V., Isaksen, L., Kallberg, P., Köhler, M., Matricardi, M., Mcnally, A.P., Monge-Sanz, B.M., Morcrette, J.J., Park, B.K., Peubey, C., de Rosnay, P., Tavolato, C., Thépaut, J.N., Vitart, F., 2011. The ERA-Interim reanalysis: configuration and performance of the data assimilation system. Q. J. R. Meteorol. Soc. 137, 553–597. https://doi.org/10.1002/qj.828.
Déqué, M., 2007. Frequency of precipitation and temperature extremes over France in an anthropogenic scenario: model results and statistical correction according to observed values. Global Planet. Change 57, 16–26. https://doi.org/10.1016/j.gloplacha.2006.11.030.
Dirks, K.N., Hay, J.E., Stow, C.D., Harris, D., 1998. High-resolution studies of rainfall on Norfolk Island. Part II: interpolation of rainfall data. J. Hydrol. 208, 187–193. https://doi.org/10.1016/S0022-1694(98)00155-3.
Dodson, R., Marks, D., 1997. Daily air temperature interpolation at high spatial resolution over a large mountainous region. Clim. Res. 8, 1–20. https://doi.org/10.3354/cr008001.
Ehret, U., Zehe, E., Wulfmeyer, V., Warrach-Sagi, K., Liebert, J., 2012. HESS Opinions "Should we apply bias correction to global and regional climate model data? Hydrol. Earth Syst. Sci. Discuss. 9, 5355–5387. https://doi.org/10.5194/hessd-9-5355-2012.
Forthofer, J.M., Butler, B.W., Wagenbrenner, N.S., 2014. A comparison of three approaches for simulating fine-scale surface winds in support of wildland fire management. Part I. Model formulation and comparison against measurements. Int. J. Wildland Fire 23, 969–981.
Garnier, B.J., Ohmura, A., 1968. A method of calculating the direct shortwave radiation income of slopes. J. Appl. Meteorol. 7, 796–800. https://doi.org/10.1175/1520-0450(1968)007<0796:AMOCTD>2.0.CO;2.
Glotter, M., Elliott, J., McInerney, D., Best, N., Foster, I., Moyer, E.J., 2014. Evaluating the utility of dynamical downscaling in agricultural impacts projections. Proc. Natl. Acad. Sci. Unit. States Am. 111, 8776–8781. https://doi.org/10.1073/pnas.1314787111.
Gobiet, A., Suklitsch, M., Heinrich, G., 2015. The effect of empirical-statistical correction of intensity-dependent model errors on the temperature climate change signal. Hydrol. Earth Syst. Sci. 19, 4055–4066. https://doi.org/10.5194/hess-19-4055-2015.
Goovaerts, P., 2000. Geostatistical approaches for incorporating elevation into the spatial interpolation of rainfall. J. Hydrol. 228, 113–129. https://doi.org/10.1016/S0022-1694(00)00144-X.
Gräler, B., Pebesma, E., Heuvelink, G., 2016. Spatio-temporal interpolation using gstat. Rev. Javer. 8, 204–218.
Granier, A., Reichstein, M., Bréda, N., Janssens, I.A., Falge, E., Ciais, P., Grünwald, T., Aubinet, M., Berbigier, P., Bernhofer, C., Buchmann, N., Facini, O., Grassi, G., Heinesch, B., Ilvesniemi, H., Keronen, P., Knohl, A., Köstner, B., Lagergren, F., Lindroth, A., Longdoz, B., Loustau, D., Mateus, J., Montagnani, L., Nys, C., Moors, E., Papale, D., Peiffer, M., Pilegaard, K., Pita, G., Pumpanen, J., Rambal, S., Rebmann, C., Rodrigues, A., Seufert, G., Tenhunen, J., Vesala, T., Wang, Q., 2007. Evidence for soil water control on carbon and water dynamics in European forests during the extremely dry year: 2003. Agric. For. Meteorol. 143, 123–145. https://doi.org/10.1016/j.agrformet.2006.12.004.
Gudmundsson, L., 2016. Qmap: Statistical Transformations for Post-processing Climate Model Output. R package version 1.0-4.
Gudmundsson, L., Bremnes, J.B., Haugen, J.E., Engen-Skaugen, T., 2012. Technical Note:

downscaling RCM precipitation to the station scale using statistical transformations - a comparison of methods. Hydrol. Earth Syst. Sci. 16, 3383–3390. https://doi.org/10.5194/hess-16-3383-2012.
Hanel, M., Kožín, R., Heřmanovský, M., Roub, R., 2017. An R package for assessment of statistical downscaling methods for hydrological climate change impact studies. Environ. Model. Software 95, 22–28. https://doi.org/10.1016/j.envsoft.2017.03.036.
Harris, R.M.B., Grose, M.R., Lee, G., Bindoff, N.L., Porfirio, L.L., Fox-Hughes, P., 2014. Climate projections for ecologists. Wiley Interdiscip. Rev. Clim. Chang. 5, 621–637. https://doi.org/10.1002/wcc.291.
Hempel, S., Frieler, K., Warszawski, L., Schewe, J., Piontek, F., 2013. A trend-preserving bias correction - the ISI-MIP approach. Earth Syst. Dyn. 4, 219–236. https://doi.org/10.5194/esd-4-219-2013.
Hijmans, R.J., Cameron, S.E., Parra, J.L., Jones, P.G., Jarvis, A., 2005. Very high resolution interpolated climate surfaces for global land areas. Int. J. Climatol. 25, 1965–1978. https://doi.org/10.1002/joc.1276.
Hofer, M., Mölg, T., Marzeion, B., Kaser, G., 2010. Empirical-statistical downscaling of reanalysis data to high-resolution air temperature and specific humidity above a glacier surface (Cordillera Blanca, Peru). J. Geophys. Res. 115, 1–15. https://doi.org/10.1029/2009JD012556.
Iannone, R., 2015. stationaRy: Get Hourly Meteorological Data from Global Stations. R package version 0.4.1.
Jacob, D., Petersen, J., Eggert, B., Alias, A., Bøssing, O., Bouwer, L.M., Braun, A., Colette, A., Georgopoulou, E., Gobiet, A., Menut, L., Nikulin, G., Haensler, A., Kriegsmann, A., Martin, E., Meijgaard, Van, E., Moseley, C., Pfeifer, S., 2014. EURO-CORDEX: new high-resolution climate change projections for European impact research. Reg. Environ. Change 14, 563–578. https://doi.org/10.1007/s10113-013-0499-2.
Kendon, E.J., Roberts, N.M., Senior, C.A., Roberts, M.J., 2012. Realism of rainfall in a very high-resolution regional climate model. J. Clim. 25, 5791–5806. https://doi.org/10.1175/JCLI-D-11-00562.1.
Kotlarski, S., Keuler, K., Christensen, O.B., Colette, A., Déqué, M., Gobiet, A., Goergen, K., Jacob, D., Lüthi, D., Van Meijgaard, E., Nikulin, G., Schär, C., Teichmann, C., Vautard, R., Warrach-Sagi, K., Wulfmeyer, V., 2014. Regional climate modeling on European scales: a joint standard evaluation of the EURO-CORDEX RCM ensemble. Geosci. Model Dev. 7, 1297–1333. https://doi.org/10.5194/gmd-7-1297-2014.
Li, J., Heap, A.D., 2014. Spatial interpolation methods applied in the environmental sciences: a review. Environ. Model. Software 53, 173–189. https://doi.org/10.1016/j.envsoft.2013.12.008.
Liston, G.E., Elder, K., 2006. A meteorological distribution system for high-resolution terrestrial modeling (MicroMet). J. Hydrometeorol. 7, 217–234. https://doi.org/10.1175/JHM486.1.
Maraun, D., Huth, R., Gutiérrez, J.M., Martín, D.S., Dubrovsky, M., Fischer, A., Hertig, E., Soares, P.M.M., Bartholy, J., Pongrácz, R., Widmann, M., Casado, M.J., Ramos, P., Bedia, J., 2017a. The VALUE perfect predictor experiment: evaluation of temporal variability. Int. J. Climatol. https://doi.org/10.1002/joc.5222.
Maraun, D., Shepherd, T.G., Widmann, M., Zappa, G., Walton, D., Gutiérrez, J.M., Hagemann, S., Richter, I., Soares, P.M.M., Hall, A., Mearns, L.O., 2017b. Towards process-informed bias correction of climate change simulations. Nat. Clim. Change 7, 764–773. https://doi.org/10.1038/nclimate3418.
Maraun, D., Wetterhall, F., Chandler, R.E., Kendon, E.J., Widmann, M., Brienen, S., Rust, H.W., Sauter, T., Themeßl, M., Venema, V.K.C., Chun, K.P., Goodess, C.M., Jones, R.G., Onof, C., Vrac, M., Thiele-Eich, I., 2010. Precipitation downscaling under climate change: recent developements to bridge the gap between dynamical models and the end user. Rev. Geophys. 48, 1–38. https://doi.org/10.1029/2009RG000314.1.INTRODUCTION.
Martin-Vide, J., 2004. Spatial distribution of a daily precipitation concentration index in peninsular Spain. Int. J. Climatol. 24, 959–971. https://doi.org/10.1002/joc.1030.
McMahon, T.A., Peel, M.C., Lowe, L., Srikanthan, R., McVicar, T.R., 2013. Estimating actual, potential, reference crop and pan evaporation using standard meteorological data: a pragmatic synthesis. Hydrol. Earth Syst. Sci. 17, 1331–1363. https://doi.org/10.5194/hess-17-1331-2013.
Mouillot, F., Rambal, S., Joffre, R., 2002. Simulating climate change impacts on fire frequency and vegetation dynamics in a Mediterranean-type ecosystem. Global Change Biol. 8, 423–437.
Palma, J., 2017. Resource communication: CliPick – climate change web picker. A tool bridging daily climate needs in process based modelling in forestry and agriculture. For. Syst. 26 eRC01.
Patsiou, T.S., Conti, E., Zimmermann, N.E., Theodoridis, S., Randin, C.F., 2014. Topo-climatic microrefugia explain the persistence of a rare endemic plant in the Alps during the last 21 millennia. Global Change Biol. 20, 2286–2300. https://doi.org/10.1111/gcb.12515.
Pierce, D., 2017. ncdf4: Interface to Unidata NetCDF (Version 4 or Earlier) Format Data Files. R package version 1.16. https://CRAN.R-project.org/package=ncdf4.
Randin, C.F., Engler, R., Normand, S., Zappa, M., Zimmermann, N.E., Pearman, P.B., Vittoz, P., Thuiller, W., Guisan, A., 2009. Climate change and plant distribution: local models predict high-elevation persistence. Global Change Biol. 15, 1557–1569. https://doi.org/10.1111/j.1365-2486.2008.01766.x.
Rössler, O., Fischer, A.M., Huebener, H., Maraun, D., Benestad, R.E., Christodoulides, P., Soares, P.M.M., Cardoso, R.M., Pagé, C., Kanamaru, H., Kreienkamp, F., Vlachogiannis, D., 2017. Challenges to link climate change data provision and user needs - perspective from the COST-action VALUE. Int. J. Climatol. https://doi.org/10.1002/joc.5060.
Ruffault, J., Martin-StPaul, N.K., Duffet, C., Goge, F., Mouillot, F., 2014. Projecting future drought in Mediterranean forests: bias correction of climate models matters!. Theor. Appl. Climatol. 117, 113–122. https://doi.org/10.1007/s00704-013-0992-z.
Ruffault, J., Martin-StPaul, N.K., Rambal, S., Mouillot, F., 2013. Differential regional responses in drought length, intensity and timing to recent climate changes in a Mediterranean forested ecosystem. Climatic Change 117, 103–117. https://doi.org/10.1007/s10584-012-0559-5.
Spitters, C.J.T., Toussaint, H.A.J.M., Goudriaan, J., 1986. Separating the diffuse and direct components of global radiation and its implications for modeling canopy photosynthesis. I. Components of incoming radiation. Agric. For. Meteorol. 38, 231–242. https://doi.org/10.1016/0168-1923(86)90060-2.
Sunyer, M.A., Hundecha, Y., Lawrence, D., Madsen, H., Willems, P., Bürger, G., Kriaučiūnienė, J., Loukas, A., Martinkova, M., Osuch, M., Vasiliades, L., von Christierson, B., Vormoor, K., Yücel, I., 2015. Inter-comparison of statistical downscaling methods for projection of extreme precipitation in Europe. Hydrol. Earth Syst. Sci. 19, 1827–1847. https://doi.org/10.5194/hess-19-1827-2015.
Tabios III, G.Q., Salas, J.D., 1985. A comparative analysis of techniques for spatial interpolation of precipitation. Water Resour. Bull. 21, 365–380.
Themeßl, M.J., Gobiet, A., Heinrich, G., 2012. Empirical-statistical downscaling and error correction of regional climate models and its impact on the climate change signal. Climatic Change 112, 449–468. https://doi.org/10.1007/s10584-011-0224-4.
Themeßl, M.J., Gobiet, A., Leuprecht, A., 2011. Empirical-statistical downscaling and error correction of daily precipitation from regional climate models. Int. J. Climatol. 31, 1530–1544. https://doi.org/10.1002/joc.2168.
Thornton, P.E., Running, S.W., 1999. An improved algorithm for estimating incident daily solar radiation from measurements of temperature, humidity, and precipitation. Agric. For. Meteorol. 93, 211–228. https://doi.org/10.1016/S0168-1923(98)00126-9.
Thornton, P.E., Running, S.W., White, M. a., 1997. Generating surfaces of daily meteorological variables over large regions of complex terrain. J. Hydrol. 190, 214–251. https://doi.org/10.1016/S0022-1694(96)03128-9.
Tomas-Burguera, M., Jiménez-Castañeda, A., Luna-Rico, M.Y., Morata, A., Vicente-Serrano, S.M., Gonzalez-Hidalgo, J.C., Beguería, S., 2016. Control de calidad de siete variables. In: X Congreso Internacional AEC: Clima, Sociedad. Riesgos Y Ordenación Del Territorio.
Turco, M., Marcos, R., Quintana-Seguí, P., Llasat, M.C., 2014. Testing instrumental and downscaled reanalysis time series for temperature trends in NE of Spain in the last century. Reg. Environ. Change 14, 1811–1823. https://doi.org/10.1007/s10113-012-0363-9.
Turco, M., Sanna, A., Herrera, S., José, M.L., Gutiérrez, M., 2013. Large biases and inconsistent climate change signals in ENSEMBLES regional projections. Climatic Change 120, 859–869. https://doi.org/10.1007/s10584-013-0844-y.
Villanueva, J.A., 2004. Tercer inventario forestal nacional (1997–2007). Ministerio de Medio Ambiente y Medio Rural. ICONA, Madrid.
Wagner, P.D., Fiener, P., Wilken, F., Kumar, S., Schneider, K., 2012. Comparison and evaluation of spatial interpolation schemes for daily rainfall in data scarce regions. J. Hydrol. 464–465, 388–400. https://doi.org/10.1016/j.jhydrol.2012.07.026.
Weedon, G.P., Gomes, S., Viterbo, P., Shuttleworth, W.J., Blyth, E., Österle, H., Adam, J.C., Bellouin, N., Boucher, O., Best, M., 2011. Creation of the WATCH forcing data and its use to assess global and regional reference crop evaporation over land during the twentieth century. J. Hydrometeorol. 12, 823–848. https://doi.org/10.1175/2011JHM1369.1.
Winkler, J.A., Guentchev, G.S., Tan, P., 2011. Climate scenario development and applications for local/regional climate change impact assessments : an overview for the non-climate scientist Part I : scenario development using downscaling methods. Geogr. Compass 6, 275–300.
Zhang, X., Srinivasan, R., 2009. GIS-based spatial precipitation estimation: a comparison of geostatistical approaches. J. Am. Water Resour. Assoc. 45, 894–906. https://doi.org/10.1111/j.1752-1688.2009.00335.x.